FIGURE 1

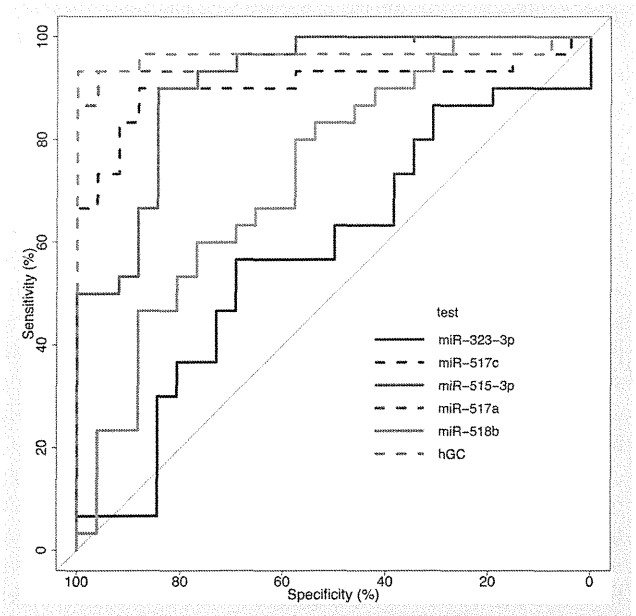

Receiver operator characteristic curve analysis using plasma pregnancy-associated miRNAs and serum hCG profiles for discriminating ectopic pregnancy/spontaneous abortion from normal pregnancy. Plasma pregnancy-associated miRNAs and serum hCG profiles (SA = spontaneous abortion, n = 12; EP = ectopic pregnancy, n = 18; NP = normal pregnancy, n = 26); miR-518b, miR-517a, miR-515-3p, miR-517c, miR-323-3p, and serum hCG yielded areas under the curve (AUC) of 0.7372 (95% CI, 0.6046–0.8698), 0.9654 (95% CI, 0.9172–1.0000), 0.9141 (95% CI, 0.8405–0.9877), 0.9077 (95% CI, 0.8192–0.9962), 0.5821 (95% CI, 0.4279–0.7362), and 0.9654 (95% CI, 0.9046–1.0000), respectively.

Miura. Ectopic pregnancy-associated miRNAs. Fertil Steril 2015.

FIGURE 2

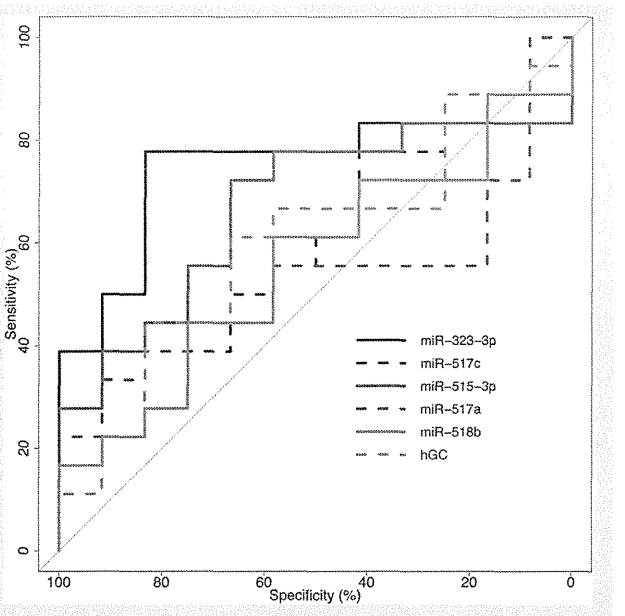

Receiver operator characteristic curve analysis using plasma pregnancy-associated miRNAs and serum hCG profiles for discriminating ectopic pregnancy from spontaneous abortion. Plasma pregnancy-associated miRNAs and serum hCG profiles (SA = spontaneous abortion, n = 12; EP = ectopic pregnancy, n = 18; NP = normal pregnancy, n = 26); miR-518b, miR-517a, miR-515-3p, miR-517c, miR-323-3p, and serum hCG yielded areas under the curve (AUC) of 0.5602 (95% CI, 0.3479–0.7725), 0.5278 (95% CI, 0.3118–0.7438), 0.6713 (95% CI, 0.4710–0.8716), 0.5972 (95% CI, 0.3873–0.8072), 0.7454 (95% CI, 0.5558–0.9349), and 0.6019 (95% CI, 0.3902–0.8135), respectively.

Miura. Ectopic pregnancy-associated miRNAs. Fertil Steril 2015.

samples from women with EP/SA compared with plasma samples from women with NP.

This finding is consistent with previously reported data regarding cell-free pregnancy-associated placenta-specific miRNAs (miR-517a, miR-519d, and miR-525-3p) in EP (4). A source of cell-free pregnancy-associated placenta-specific miRNAs in maternal plasma is the villous trophoblast, which can release exosomes containing miRNAs into the maternal circulation (11, 12). The placenta-specific miRNAs (miR-515-3p, miR-517a, and miR-517c) analyzed in this study were located in the C19MC region, which is imprinted in the placenta with expression from the paternally inherited chromosome (17). MicroRNAs are small, nonprotein coding RNAs (21–25 nucleotides) that function as regulators of gene expression by antisense complimentarily to specific messenger RNAs (18–20). Therefore, our results suggest that the circulating levels of cell-free pregnancy-associated placenta-specific miRNAs from the C19MC region in maternal plasma may reflect the functional status of the villi, and that these molecules in plasma samples have potential as molecular markers for discriminating abnormal placentation (or nonviable pregnancy) from normal placentation (or viable pregnancy) in the first trimester.

Plasma concentrations of cell-free pregnancy-associated but not placenta-specific miRNA (miR-323-3p) have been confirmed to have significantly different plasma concentrations in women with EP, SA, or NP. We could also confirm the previously reported data that miR-323-3p was the candidate marker that showed a significant difference among the three groups (4). Additionally, a previous study reported higher circulating levels of miR-323-3p in an EP group relative to SA and NP groups (4), and our study showed that the plasma concentrations of cell-free miR-323-3p could distinguish EP from SA, yielding the highest AUC, which suggests that the circulating level of cell-free miR-323-3p in plasma is one of potential biomarkers for the diagnosis of EP.

However, because of the small sample size, our data showed no statistically significant difference in plasma concentrations of cell-free miR-323-3p between the EP and SA groups, or between the EP and NP groups. In our study, the SA group included two cases of pregnancy of unknown location, which indicates a situation of complete abortion or early EP loss. Therefore, it is possible that our study could not detect a statistically significant difference in circulating miR-323-3p levels between the EP and SA groups.

Furthermore, Lozoya et al. (21) reported that the expression of miR-323-3p is lower in EP tissues than in normal human embryonic tissues at 7 to 9 weeks of gestation. Our

previous study also identified miR-323-3p as a pregnancy-associated miRNA in maternal plasma (7). The expression pattern of miR-323-3p, which is located on the chromosome 14 miRNA cluster region (C14MC), is imprinted in embryonic and placental tissues, and in adults is restricted to the brain with expression from the maternally inherited chromosome (22). Thus, in maternal plasma during the first trimester, the source of circulating miR-323-3p on C14MC seems to be of maternal origin from brain tissue of the pregnant women herself, and of fetal origin from embryonic and villus tissues. Depending on the specifics of each case of EP, the ratio of villus and embryonic tissues in pregnant products can vary, and the imprinting status in tissues in women with EP may also vary. Also, EP is an emergency condition that can prompt a variety of problems in pregnant women, so various factors from the pregnant woman also may influence the circulating levels of miR-323-3p on C14MC in plasma.

In consequence, the small sample size in our study and other studies may be the reason for the discrepancy regarding circulating levels of cell-free miR-323-3p among the studies (4, 21). A larger study is necessary to determine whether cell-free miR-323-3p is a universal biomarker for the identification of EP (4).

Subsequently, we analyzed the diagnostic value of circulating pregnancy-associated miRNAs levels in plasma for the identification of EP. The correction coefficient analysis showed no association between the serum concentration of hCG and the plasma concentration of cell-free pregnancy-associated miRNAs in pregnant women, suggesting that cell-free pregnancy-associated miRNAs may be independent of serum hCG as a biomarker for EP (see Table 2). The ROC curve analysis revealed that four single pregnancy-associated placenta-specific miRNAs (miR-517a, miR-517c, miR-518b, and miR-515-3p) in plasma could discriminate EP/SA from NP, yielding high AUCs (see Fig. 1). Furthermore, the plasma concentrations of cell-free miR-323-3p could distinguish EP from SA, yielding the highest AUC.

Serum hCG is currently used as a biomarker for early pregnancy; it can be measured simply and noninvasively, and it can serve as a useful indicator of pregnant status (1–3). However, the sensitivity and positive predictive values of serum hCG level are relatively low for detecting EP (1–4). In our analysis, which used the independent population of a previous study (4), we were able to confirm that pregnancy-associated miRNAs are differentially expressed in EP and NP. Moreover, plasma cell-free pregnancy-associated miRNAs are a possible independent marker of serum hCG.

As for the possible clinical application of pregnancy-associated miRNAs for the diagnosis of EP, the plasma concentration of cell-free pregnancy-associated placenta-specific miRNAs (miR-517a, miR-517c, miR-518b, and miR-515-3p on C19MC) discriminates EP/SA from NP, so the plasma concentrations of cell-free miR-323-3p on C14MC could distinguish between EP and SA. Thus, the advent of a noninvasive predictive procedure using maternal plasma concentrations of cell-free pregnancy-associated miRNAs would undoubtedly be a great advance in the clinical management of abnormal pregnancies in the first trimester. This measurement could allow obstetricians and gynecologists to discriminate EP from SA/NP in early gestation.

Cell-free pregnancy-associated miRNA measurements combined with an ultrasonographic examination and serial quantitative hCG tests could be used to generate a noninvasive diagnosis of EP. In turn, this could result in a reduction in perinatal maternal mortality not only from EP but also from other conditions of abnormal placentation, including placenta previa and abruption placenta. However, it should be noted that our study was performed on EP that was already sufficiently advanced to be diagnosed via ultrasound (6–10 weeks of gestation). It is not clear whether pregnancy-associated miRNAs are expressed at an earlier stage of EP (before 6 weeks of gestation). Therefore, further study should confirm whether pregnancy-associated miRNAs are useful to diagnosis early EP.

In conclusion, we confirmed the clinical significance of cell-free pregnancy-associated miRNAs (miR-517a, miR-517c, miR-518b, and miR-515-3p on C19MC and miR-323-3p on C14 MC) in plasma as potential biomarkers for the diagnosis of ectopic pregnancies. Circulating levels of cell-free pregnancy-associated placenta specific miRNAs in plasma can distinguish EP/SA from NP with high accuracy. Compared with serum hCG levels, the circulating levels of cell-free miR-323-3p in plasma can distinguish EP from SA with higher accuracy. Although our data are still preliminary because of our small sample size, the measurement of cell-free pregnancy-associated miRNAs in plasma has potential as a diagnostic and a follow-up test for EP. Future studies on the biologic pathway of cell-free pregnancy-associated miRNAs in plasma may contribute to the elucidation of the molecular pathogenesis of EP (23) and the discovery of targets to prevent EP.

REFERENCES

1. Barnhart KT. Clinical practice. Ectopic pregnancy. N Engl J Med 2009;361:379–87.
2. Farquhar CM. Ectopic pregnancy. Lancet 2005;366:583–91.
3. American College of Obstetricians Gynecologists. ACOG Practice Bulletin No. 94: medical management of ectopic pregnancy. Obstet Gynecol 2008;111:1479–85.
4. Zhao Z, Zhao Q, Warrick J, Lockwood CM, Woodworth A, Moley KH, et al. Circulating microRNA miR-323-3p as a biomarker of ectopic pregnancy. Clin Chem 2012;58:896–905.
5. Chim SS, Shing TK, Hung EC, Leung TY, Lau TK, Chiu RW, et al. Detection and characterization of placental microRNAs in maternal plasma. Clin Chem 2008;54:482–90.
6. Chiu RW, Lo YM. Pregnancy-associated microRNAs in maternal plasma: a channel for fetal-maternal communication? Clin Chem 2010;56:1656–7.
7. Miura K, Miura S, Yamasaki K, Higashijima A, Kinoshita A, Yoshiura K, et al. Identification of pregnancy-associated microRNAs in maternal plasma. Clin Chem 2010;56:1767–71.
8. Ng EK, Tsui NB, Lau TK, Leung TN, Chiu RW, Panesar NS, et al. mRNA of placental origin is readily detectable in maternal plasma. Proc Natl Acad Sci U S A 2003;100:4748–53.
9. Heung MM, Jin S, Tsui NB, Ding C, Leung TY, Lau TK, et al. Placenta-derived fetal specific mRNA is more readily detectable in maternal plasma than in whole blood. PLoS One 2009;4:e5858.
10. Chiu RW, Poon LL, Lau TK, Leung TN, Wong EM, Lo YM. Effects of blood-processing protocols on fetal and total DNA quantification in maternal plasma. Clin Chem 2001;47:1607–13.

11. Donker RB, Mouillet JF, Chu T, Hubel CA, Stolz DB, Morelli AE, et al. The expression profile of C19MC microRNAs in primary human trophoblast cells and exosomes. Mol Hum Reprod 2012;18:417–24.
12. Luo SS, Ishibashi O, Ishikawa G, Ishikawa T, Katayama A, Mishima T, et al. Human villous trophoblasts express and secrete placenta-specific microRNAs into maternal circulation via exosomes. Biol Reprod 2009;81:717–29.
13. Higashijima A, Miura K, Mishima H, Kinoshita A, Jo O, Abe S, et al. Characterization of placenta-specific microRNAs in fetal growth restriction pregnancy. Prenat Diagn 2013;33:214–22.
14. Hasegawa Y, Miura K, Furuya K, Yoshiura KI, Masuzaki H. Identification of complete hydatidiform mole pregnancy-associated microRNAs in plasma. Clin Chem 2013;59:1410–2.
15. Ng EK, Tsui NB, Lam NY, Chiu RW, Yu SC, Wong SC, et al. Presence of filterable and nonfilterable mRNA in the plasma of cancer patients and healthy individuals. Clin Chem 2002;48:1212–7.
16. Robin X, Turck N, Hainard A, Tiberti N, Lisacek F, Sanchez J-C, et al. pROC: an open-source package for R and S+ to analyze and compare ROC curves. BMC Bioinformatics 2011;12:77.
17. Noguer-Dance M, Abu-Amero S, Al-Khtib M, Lefèvre A, Coullin P, Moore GE, et al. The primate-specific microRNA gene cluster (C19MC) is imprinted in the placenta. Hum Mol Genet 2010;19:3566–82.
18. Lee RC, Feinbaum RL, Ambros V. The C. elegans heterochronic gene lin-4 encodes small RNAs with antisense complementarity to lin-14. Cell 1993; 75:843–54.
19. Mendell JT. MicroRNAs: critical regulators of development, cellular physiology and malignancy. Cell Cycle 2005;4:1179–84.
20. Plasterk RH. Micro RNAs in animal development. Cell 2006;124: 877–81.
21. Lozoya T, Domínguez F, Romero-Ruiz A, Steffani L, Martínez S, Monterde M, et al. The Lin28/Let-7 system in early human embryonic tissue and ectopic pregnancy. PLoS One 2014;9:e87698.
22. Morales-Prieto DM, Ospina-Prieto S, Chaiwangyen W, Schoenleben M, Markert UR. Pregnancy-associated miRNA-clusters. J Reprod Immunol 2013;97:51–61.
23. Galliano D, Pellicer A. MicroRNA and implantation. Fertil Steril 2014;101: 1531–44.

SUPPLEMENTAL FIGURE 1

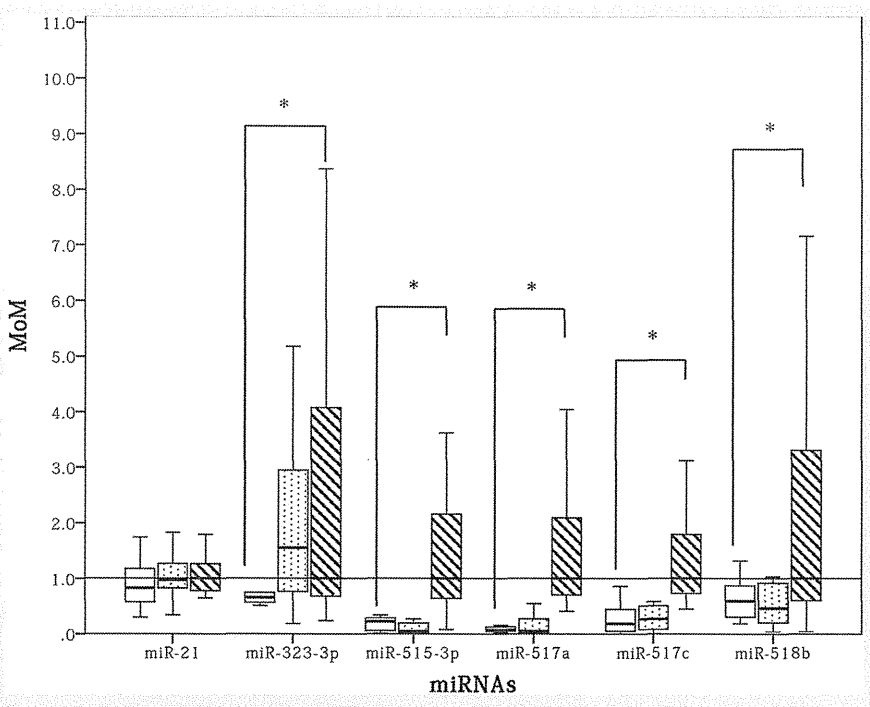

Circulating levels of plasma cell-free pregnancy-associated placenta-specific miRNAs in spontaneous abortion, ectopic pregnancy, and normal pregnancy groups. Circulating levels were expressed as multiple of median (MoM) values. *White bars* indicate data from the spontaneous abortion group, *dot-pattern bars* indicate data from the ectopic pregnancy group, and *hatched bars* indicate the data from the normal pregnancy group. Circulating levels of miRNAs in maternal plasma are expressed as MoM values. *Statistically significant differences (Kruskal-Wallis test, $P<.05$).

Miura. Ectopic pregnancy-associated miRNAs. Fertil Steril 2015.

CLINICAL GENETICS An International Journal of Genetics, Molecular and Personalized Medicine

Clin Genet 2015: 88: 261–266
Printed in Singapore. All rights reserved

CLINICAL GENETICS
doi: 10.1111/cge.12496

Short Report

Autosomal recessive cystinuria caused by genome-wide paternal uniparental isodisomy in a patient with Beckwith–Wiedemann syndrome

Ohtsuka Y, Higashimoto K, Sasaki K, Jozaki K, Yoshinaga H, Okamoto N, Takama Y, Kubota A, Nakayama M, Yatsuki H, Nishioka K, Joh K, Mukai T, Yoshiura K-i, Soejima H. Autosomal recessive cystinuria caused by genome-wide paternal uniparental isodisomy in a patient with Beckwith–Wiedemann syndrome.
Clin Genet 2015: 88: 261–266. © John Wiley & Sons A/S. Published by John Wiley & Sons Ltd, 2014

Approximately 20% of Beckwith–Wiedemann syndrome (BWS) cases are caused by mosaic paternal uniparental disomy of chromosome 11 (pUPD11). Although pUPD11 is usually limited to the short arm of chromosome 11, a small minority of BWS cases show genome-wide mosaic pUPD (GWpUPD). These patients show variable clinical features depending on mosaic ratio, imprinting status of other chromosomes, and paternally inherited recessive mutations. To date, there have been no reports of a mosaic GWpUPD patient with an autosomal recessive disease caused by a paternally inherited recessive mutation. Here, we describe a patient concurrently showing the clinical features of BWS and autosomal recessive cystinuria. Genetic analyses revealed that the patient has mosaic GWpUPD and an inherited paternal homozygous mutation in *SLC7A9*. This is the first report indicating that a paternally inherited recessive mutation can cause an autosomal recessive disease in cases of GWpUPD mosaicism. Investigation into recessive mutations and the dysregulation of imprinting domains is critical in understanding precise clinical conditions of patients with mosaic GWpUPD.

Conflict of interest

The authors have no competing financial interests to declare.

Y. Ohtsuka[a], K. Higashimoto[a], K. Sasaki[b], K. Jozaki[a], H. Yoshinaga[a], N. Okamoto[c], Y. Takama[d], A. Kubota[d], M. Nakayama[e], H. Yatsuki[a], K. Nishioka[a], K. Joh[a], T. Mukai[f], K.-i. Yoshiura[b] and H. Soejima[a]

[a]Division of Molecular Genetics and Epigenetics, Department of Biomolecular Sciences, Faculty of Medicine, Saga University, Saga, Japan, [b]Department of Human Genetics, Nagasaki University Graduate School of Biomedical Sciences, Nagasaki, Japan, [c]Department of Medical Genetics , [d]Department of Pediatric Surgery , [e]Department of Pathology, Osaka Medical Center and Research Institute for Maternal and Child Health, Osaka, Japan, and [f]Nishikyushu University, Saga, Japan

Key words: Beckwith–Wiedemann syndrome – cystinuria – genome-wide paternal uniparental disomy mosaicism – *SLC3A1* – *SLC7A9*

Corresponding author: Hidenobu Soejima, Division of Molecular Genetics and Epigenetics, Department of Biomolecular Sciences, Faculty of Medicine, Saga University, 5-1-1 Nabeshima, Saga 849-8501, Japan.
Tel.: +81 952 34 2260;
fax: +81 952 34 2067;
e-mail: soejimah@med.saga-u.ac.jp

Received 8 July 2014, revised and accepted for publication 27 August 2014

Beckwith–Wiedemann syndrome (BWS) (OMIM #130650) is an imprinting disorder characterized by peculiar prenatal and postnatal macrosomia, macroglossia, and abdominal wall defects. There are various genetic and epigenetic abnormalities that can cause BWS, although paternal uniparental disomy of 11p15 (pUPD11) accounts for around 20% of cases (1, 2). The minimum pUPD size is approximately 2.7 Mb from

the telomere of 11p, including both imprinting control regions, *H19*DMR and *Kv*DMR1 (3). pUPD11 causes hypermethylation of *H19*DMR and hypomethylation of *Kv*DMR1, which leads to overexpression of *IGF2* and reduced expression of *H19* and *CDKN1C*. In its most wide-reaching variety, pUPD acts on the whole genome, and is denoted as genome-wide pUPD (GWpUPD). Non-mosaic GWpUPD results in the formation of a hydatidiform mole, while individuals with GWpUPD mosaicism are born alive (2). GWpUPD patients usually show clinical features of BWS and other variable features thought to depend on the mosaic ratio, the imprinting status of other chromosomes such as chromosomes 6, 14, 15, and 20 (pUPDs of these chromosomes cause other imprinting disorders), and paternally inherited recessive mutations (4). However, to date, there have been no reports of a mosaic GWpUPD patient with an autosomal recessive disease caused by a paternally inherited recessive mutation.

Cystinuria (OMIM #220100) is an autosomal recessive disorder characterized by impaired epithelial cell transport of cystine and dibasic amino acids (lysine, ornithine, and arginine) in the proximal renal tubule and gastrointestinal tract. The impaired renal reabsorption and the low solubility of cystine cause the formation of calculi in the urinary tract (5). Causative genes for cystinuria include *SLC3A1* and *SLC7A9*. These genes encode proteins that comprise the rBAT/$b^{0,+}$AT heterodimer, which mediates the exchange of extracellular cationic amino acids and cystine for intracellular neutral amino acids (6).

We investigated a patient with clinical features of both BWS and cystinuria. Genetic analyses revealed that the patient harbored mosaic GWpUPD and inherited a homozygous mutation of *SLC7A9* paternally. This is the first reported case of a patient with these features exhibited concurrently.

Materials and methods

Patient report

The female infant with a karyotype of 46,XX was the first-born baby to non-consanguineous, healthy, Japanese parents after 34 weeks and 6 days of gestation. Her birth weight was 4254 g [+6.8 SD (standard deviation)], and she exhibited omphalocele, macroglossia, and nevus flammeus on her forehead. These conditions satisfy the diagnostic criteria for BWS as described by Weksberg et al. (7). After birth, she also manifested persistent hyperinsulinemic hypoglycemia and an extremely high level of serum alpha-fetoprotein (300,000 ng/ml). She was diagnosed with diffuse nesidioblastosis in the pancreatic body, and a partial pancreatectomy was performed twice, at 2 months and at 8 years of age (8). In addition, at puberty she had bilateral breast fibroadenomas and an ovarian adenofibroma, as recently reported (9). She did not develop any mental or motor delay.

Atrophy of the left kidney and enlargement of the right kidney were detected at birth, and urinary stones in the bladder and medullary calcinosis in both kidneys were detected at 10 months of age (Fig. 1). The

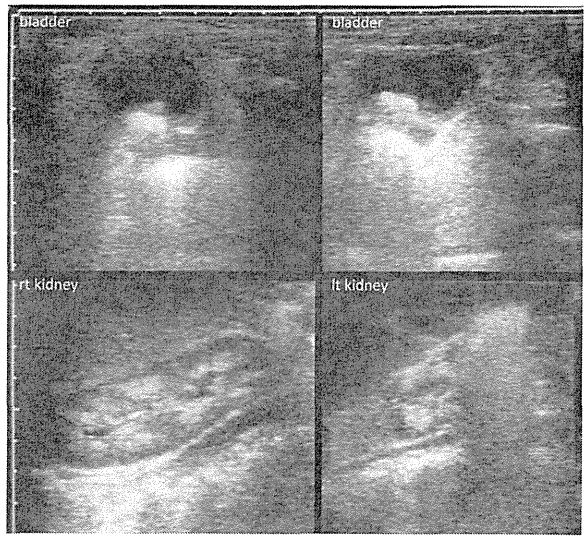

Fig. 1. Sonography of urolithiasis. Ultrasound images of the patient at one year of age shows a 1 cm stone in the bladder and medullary calcinosis in both kidneys. Atrophy of the left kidney was diagnosed at birth.

urinary amino acid analysis revealed high concentrations of cystine (551 μmol/l), lysine (5175 μmol/l), and arginine (3837 μmol/l), and cystine crystals were visible in a urine sample. Therefore, she was also diagnosed with cystinuria. Her parents had no history of urolithiasis; however, cystine and lysine in the father's urine were moderately elevated (296 μmol/l and 850 μmol/l, respectively).

This study was approved by the Ethics Committee for Human Genome and Gene Analyses of the Faculty of Medicine, Saga University.

DNA isolation

Genomic DNA was extracted from the peripheral blood of the patient and her parents, the patient's pancreas, and urine using commercially available DNA extraction kits.

SNP array analysis

Single nucleotide polymorphism (SNP) array analysis was performed with Genome-Wide Human SNP Array 5.0 (Affymetrix, Santa Clara, CA) according to the manufacturer's protocol. The genotype was analyzed using GENOTYPING CONSOLE (GTC) 4.1 software (Affymetrix). Copy number, allele ratio, and trio SNP analyses were performed using PARTEK GENOMICS SUITE version 6.6 beta (Partek Inc., St. Louis, MO). A reference generated from 89 Japanese samples was used. The genomic positions of the SNPs corresponded to GRCh37/hg19.

Mutation analyses of *SLC3A1* and *SLC7A9* genes

All coding exons and flanking intronic regions of *SLC3A1* and *SLC7A9* genes were amplified by polymerase chain reaction (PCR) and directly sequenced.

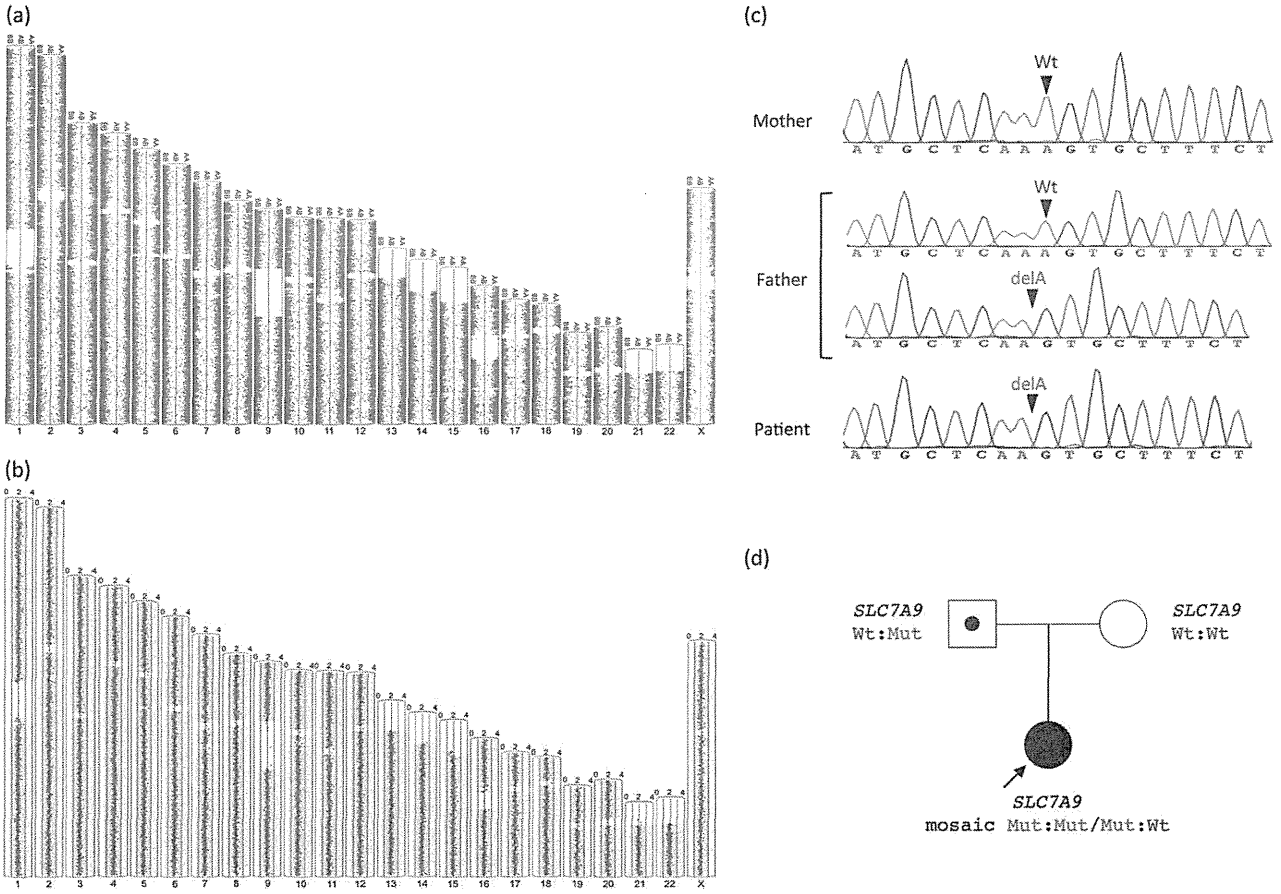

Fig. 2. Results of single nucleotide polymorphism (SNP) array analysis and mutation analysis of a cystinuria causative gene, *SLC7A9*. (**a**, **b**) Results of patient SNP array analysis. Genotyping (**a**) showed homozygous (AA or BB) results for almost all SNPs throughout all chromosomes, and absence of aberrant copy number variation (**b**); this evidence supports the notion of mosaicism for genome-wide paternal uniparental disomy (GWpUPD) of isodisomic androgenetic cells and normal biparental cells. (**c**) Results of mutation analysis of a cystinuria causative gene, *SLC7A9*. Sanger sequencing revealed a single-base deletion in exon 10 in both the father and the patient. Polymerase chain reaction (PCR)-cloning-sequencing revealed four wild-type clones and nine mutant clones in the father, indicating heterozygosity for the mutation. PCR direct sequencing showed that the patient seemed to be homozygous for the mutation because of a high mosaic ratio for GWpUPD. The mother did not have the mutation. (**d**) Patient's family pedigree. The *SLC7A9* mutation found in the patient was paternally inherited. In the patient, cells with GWpUPD were homozygous for the mutation, whereas biparental cells were heterozygous, containing both the mutation and the maternally inherited wild-type allele.

The PCR product of *SLC7A9* exon 10 in the father was cloned into a pT7Blue T-Vector (Novagen, San Diego, CA), and individual clones were sequenced. Primers for the mutation analyses are listed in Table S1, Supporting Information.

Results

To identify the potential cause of the BWS, we first performed methylation-sensitive Southern blots of two imprinting control regions at 11p15, *H19*DMR, and *Kv*DMR1. The methylation index (MI) was 99% at *H19*DMR and 2% at *Kv*DMR1 (Fig. S1). Because *H19*DMR is methylated on the paternal allele and *Kv*DMR1 is methylated on the maternal allele, pUPD of the region with a high mosaic ratio was strongly suggested.

We then performed microarray analysis of the patient, father, and mother SNP trios using SNP Array 5.0. The results showed two normal copies in the patient and her parents; however, the patient's genotype contained homozygous (AA or BB) results for almost all SNPs throughout all chromosomes (Fig. 2a,b). The genotyping of the trios indicated that the informative SNPs in the patient had been transmitted via paternal uniparental inheritance (data of chromosomes 2 and 19 are shown in Fig. S2). To calculate the mosaic ratio, we quantitatively analyzed microsatellite markers across all chromosomes except chromosome Y. In the patient, the average mosaic ratio of all informative markers was 91% in the peripheral blood and 83% in the pancreas (Table S2). These results indicated GWpUPD mosaicism of isodisomic androgenetic cells and normal biparental cells. Because mosaic GWpUPD necessarily includes 11p15.4-p15.5, we concluded that the causative abnormality for the BWS phenotype was pUPD11.

Finally, because the patient was diagnosed with autosomal recessive cystinuria, we performed mutation analyses of the supposed causative genes for cystinuria, *SLC3A1* at 2p21 and *SLC7A9* at 19q13.1. The

Table 1. Literature review of live-born patients with genome-wide paternal UPD[a]

	Our patient	Johnson et al. (13)	Kalish et al. (12)			Gogiel et al. (15)	Inbar-Feigenberg et al. (14)	Yamazawa et al. (4)	Romanelli et al. (16)	Wilson et al. (17)		Reed et al. (18)	Giurgea et al. (19)	Bryke and Garber (20)	Hoban et al. (21)
			Patient #1	Patient #2	Patient #3					Patient #1	Patient #2				
Gestational age	34 weeks 6 days	30 weeks 6 days	31 weeks 5 days	30 weeks 6 days	24 weeks 1 days	37 weeks	33 weeks	34 weeks		36 weeks	29 weeks 6 days	30 weeks 4 days	35 weeks		42 weeks
Birth weight (g)	4254	2460				3850	2270	3730	3750			1110	2260		
Weight percentile	>97th	>97th	85th	95th	50th	>90th	75th	>97th		>97th	>90th		25–50th		
Macroglossia	+			+		+		+		+					
Abdominal wall defect	+	+	+	+	+	+	+	+		+	+				
Visceromegaly	+		+	+	+	+	+	+		+	+			+	
Hemihyperplasia		+	+	+		+	+	+	+		+		+	+	+
Hypoglycemia	+	+	+	+	+	+	+	+	+	+	+		+		
Cutaneous abnormality	+		+	+			+		+		+			+	
Cardiac abnormality	+		+			+	+			+				+	
Neurological abnormality			+				+	+	+	+	+			+	
Tumor development	+		+	+	+	+	+	+	+	+	+	+	+	+	+
Failure to thrive				+				+		+	+			+	
Placental abnormality	+		+	+		+	+	+			+	+			
Other abnormality			+	+	+	+	+	+	+	+	+			+	
Features estimated paternal UPD	UPD11	UPD11	UPD11, 14	UPD11	UPD11	UPD11, 14	UPD11, 15, 20	UPD11, 14, 15	UPD11, 15	UPD11	UPD11		UPD11	UPD6, 14, 15, 20	UPD11
Other findings	Cystinuria (homozygous mutation of *SLC7A9*)	Hyperkalemia, abdominal swelling, deceased		Peripheral pulmonic stenosis, small bowel obstructions	Respiratory distress, cliteromegaly, deceased	Cerebral seizure, non-obliterating thrombosis of the inferior vena cava, multiple fractures, tachypnea	Strabismus, renal dysplasia, respiratory distress, small choroid plexus bleed, low level of 25-hydroxy vitamin D	Asphyxia	Renal stone	Respiratory insufficiency, inflammatory condition, granulocyte hyperplasia, arthritis, stenosis of arteries, hemiplegic stroke, hypertension		Fetal distress			

UPD, uniparental disomy.

[a]Cutaneous abnormality: hemangioma, cutaneous capillary vascular malformation or pigmentation. Neurological abnormality: developmental and motor delay, hypotonia, convulsion or autism. Other abnormality: ear lobe anomaly, hypertelorism, abnormal facies, bell-shaped thorax, or others.

SNP array showed two normal copies of both regions (Fig. S2). Sanger sequencing revealed a single-base deletion in exon 10 of *SLC7A9*, which led to a previously reported frameshift mutation (c.1017delA, p.V340fsX21, RefSeq: NM_001126335) (10), whereas no mutation was found in *SLC3A1* (Fig. 2c). The father was a heterozygous carrier of the mutation showing moderately elevated cystine and lysine in his urine without urolithiasis, while the mother was homozygous for the wild-type allele (Fig. 2c). The patient seemed to be homozygous for the mutation because of the high mosaic ratio of GWpUPD (Fig. 2c,d). *In silico* prediction programs such as MutationTaster (http://www.mutationtaster.org/) and SIFT-indels (http://sift.bii.a-star.edu.sg/www/SIFT_indels2.html) predicted the *SLC7A9* mutation as 'DISEASE CAUSING' and 'DAMAGING', respectively. The mutation could not be found after a comprehensive database search covering dbSNP (http://www.ncbi.nlm.nih.gov/projects/SNP/), 1000 Genomes (http://www.1000genomes.org/), ClinVar (http://www.ncbi.nlm.nih.gov/clinvar/), the Human Genome Variation Database (http://www.genome.med.kyoto-u.ac.jp/SnpDB/index.html), and the Exome Variant Server (http://evs.gs. washington.edu/EVS/). Furthermore, we identified the *SLC7A9* mutation in DNA from the patient's urine (Fig. S3b).

On the basis of these findings we concluded that the patient was homozygous for the *SLC7A9* mutation in GWpUPD cells and heterozygous in biparental cells. Because a high ratio of mosaicism was found in the patient's urine (average mosaic rate: 76%) (Fig. S3a), we speculated that the high ratio of mosaicism also occurred in the patient's kidneys, which resulted in the observed cystinuria.

Discussion

In this study, we describe a patient concurrently afflicted with BWS and autosomal recessive cystinuria. Genetic analyses revealed that the patient, who possesses mosaic GWpUPD, is also homozygous for a *SLC7A9* mutation in GWpUPD cells, while her normal biparental cells are heterozygous. The mutation was inherited from the patient's father, who carried the mutation.

Approximately 20% of patients with BWS show mosaicism for pUPD11 (1). This segmental pUPD is considered to result from mitotic recombination at an early embryonic stage (11). A small number of reports exist that detail GWpUPD patients with BWS phenotypes (1). Fifteen patients with live-born mosaic GWpUPD, including our patient, have been described so far in 11 reports (Table 1) (4, 12–21). Although previous assumptions were of low GWpUPD incidence in pUPD11 patients, a recent report suggested that GWpUPD might actually be more frequent than expected because two GWpUPD patients were found out of 11 pUPD11 patients (22). All these patients showed only one paternal haplotype (isodisomy) and no evidence of any chromosomal crossing-over. This strongly suggests that a mechanism of mosaic GWpUPD involves normal fertilization followed by failure of maternal DNA replication and paternal genome endoreplication (12, 23, 24). These patients frequently show hyperinsulinemic hypoglycemia (12/15), often accompanied by nesidioblastosis, for which partial or near-total pancreatectomy may be required. The incidence of tumor development is much higher in GWpUPD patients (14/15) than in segmental pUPD11 (approximately 25%) (Table 1) (25). Several types of benign and malignant tumors develop metachronously and ectopically (12). Because segmental pUPD11 itself is a risk factor for tumor development, there may be additional factors in GWpUPD patients, such as as-yet poorly characterized imprinted regions and undiscovered recessive loci associated with cell growth or survival (12). The possibility of GWpUPD should be tested in patients with pUPD11 as a general, in particular to guard against their increased tumor risk.

Although other chromosomes, especially chromosomes 6, 14, 15, and 20, are also pUPD in GWpUPD patients, associated clinical features were seen less frequently with them, suggesting (epi)dominance of pUPD11 (Table 1). Yamazawa et al. suggested several determination factors for clinical features of mosaic GWpUPD, including the mosaic ratios in various tissues, dysregulation of imprinted domains, and unmasking of paternally inherited recessive mutations (4).

We found that our patient was homozygous for a one-base deletion mutation of *SLC7A9*, which is a causative gene for cystinuria. A GWpUPD patient has been previously reported to have renal calcium stones. However, the cause of the renal stones remains unknown (16). *SLC7A9* encodes $b^{+,0}$AT, which is a light subunit of the rBAT/$b^{0,+}$AT amino acid transporter expressed in the renal proximal tubule (5, 6). The mutation has been reported to decrease cystine transport activity drastically compared with wild-type rBAT/$b^{0,+}$AT *in vitro* (10). The loss of function of this transporter system leads to the formation of cystine stones in patients.

In conclusion, we report for the first time a patient concurrently affected by both BWS and autosomal recessive cystinuria. The genotype of this patient clearly indicates that a paternally inherited recessive mutation can cause a recessive disease in patients with mosaic GWpUPD. To understand the clinical conditions of patients with mosaic GWpUPD better, further investigation of dysregulation of imprinted domains and recessive mutations is necessary. To this end, whole exome sequencing would be useful in identifying paternally inherited recessive mutations.

Supporting Information

Additional supporting information may be found in the online version of this article at the publisher's web-site.

Acknowledgements

This study was supported, in part, by a Grant for Research on Intractable Diseases from the Ministry of Health, Labor, and Welfare; a Grant for Child Health and Development from the National Center for Child Health and Development; a Grant-in-Aid for Challenging Exploratory Research; and a Grant-in-Aid for Scientific Research (C) from the Japan Society for the Promotion of Science.

References

1. Choufani S, Shuman C, Weksberg R. Molecular findings in Beckwith-Wiedemann syndrome. Am J Med Genet C Semin Med Genet 2013: 163C: 131–140.
2. Soejima H, Higashimoto K. Epigenetic and genetic alterations of the imprinting disorder Beckwith-Wiedemann syndrome and related disorders. J Hum Genet 2013: 58: 402–409.
3. Romanelli V, Meneses HN, Fernández L et al. Beckwith-Wiedemann syndrome and uniparental disomy 11p: fine mapping of the recombination breakpoints and evaluation of several techniques. Eur J Hum Genet 2011: 19: 416–421.
4. Yamazawa K, Nakabayashi K, Matsuoka K et al. Androgenetic/biparental mosaicism in a girl with Beckwith-Wiedemann syndrome-like and upd(14)pat-like phenotypes. J Hum Genet 2011: 56: 91–93.
5. Barbosa M, Lopes A, Mota C et al. Clinical, biochemical and molecular characterization of cystinuria in a cohort of 12 patients. Clin Genet 2012: 81: 47–55.
6. Fotiadis D, Kanai Y, Palacín M. The SLC3 and SLC7 families of amino acid transporters. Mol Aspects Med 2013: 34: 139–158.
7. Weksberg R, Shuman C, Beckwith JB. Beckwith-Wiedemann syndrome. Eur J Hum Genet 2010: 18: 8–14.
8. Kubota A, Yonekura T, Usui N et al. Two cases of persistent hyperinsulinemic hypoglycemia that showed spontaneous regression and maturation of the Langerhans islets. J Pediatr Surg 2000: 35: 1661–1662.
9. Takama Y, Kubota A, Nakayama M et al. Fibroadenoma in Beckwith–Wiedemann syndrome with paternal uniparental disomy of chromosome 11p15.5. Pediatrics International 2014: in press.
10. Shigeta Y, Kanai Y, Chairoungdua A et al. A novel missense mutation of SLC7A9 frequent in Japanese cystinuria cases affecting the C-terminus of the transporter. Kidney Int 2006: 69: 1198–1206.
11. Yamazawa K, Nakabayashi K, Kagami M et al. Parthenogenetic chimaerism/mosaicism with a Silver-Russell syndrome-like phenotype. J Med Genet 2010: 47: 782–785.
12. Kalish JM, Conlin LK, Bhatti TR et al. Clinical features of three girls with mosaic genome-wide paternal uniparental isodisomy. Am J Med Genet A 2013: 161A: 1929–1939.
13. Johnson JP, Waterson J, Schwanke C et al. Genome-wide androgenetic mosaicism. Clin Genet 2014: 85: 282–285.
14. Inbar-Feigenberg M, Choufani S, Cytrynbaum C et al. Mosaicism for genome-wide paternal uniparental disomy with features of multiple imprinting disorders: diagnostic and management issues. Am J Med Genet A 2013: 161A: 13–20.
15. Gogiel M, Begemann M, Spengler S et al. Genome-wide paternal uniparental disomy mosaicism in a woman with Beckwith-Wiedemann syndrome and ovarian steroid cell tumour. Eur J Hum Genet 2013: 21: 788–791.
16. Romanelli V, Nevado J, Fraga M et al. Constitutional mosaic genome-wide uniparental disomy due to diploidisation: an unusual cancer-predisposing mechanism. J Med Genet 2011: 48: 212–216.
17. Wilson M, Peters G, Bennetts B et al. The clinical phenotype of mosaicism for genome-wide paternal uniparental disomy: two new reports. Am J Med Genet A 2008: 146A: 137–148.
18. Reed RC, Beischel L, Schoof J et al. Androgenetic/biparental mosaicism in an infant with hepatic mesenchymal hamartoma and placental mesenchymal dysplasia. Pediatr Dev Pathol 2008: 11: 377–383.
19. Giurgea I, Sanlaville D, Fournet JC et al. Congenital hyperinsulinism and mosaic abnormalities of the ploidy. J Med Genet 2006: 43: 248–254.
20. Bryke C, Garber A, Israel J. Evolution of a complex phenotype in a unique patient with a paternal uniparental disomy for every chromosome cell line and a normal biparental inheritance cell line. Toronto, Canada: The annual meeting of The American Society of Human Genetics, 2004: Program Number: 823.
21. Hoban PR, Heighway J, White GR et al. Genome-wide loss of maternal alleles in a nephrogenic rest and Wilms' tumour from a BWS patient. Hum Genet 1995: 95: 651–656.
22. Eggermann T, Heilsberg AK, Bens S et al. Additional molecular findings in 11p15-associated imprinting disorders: an urgent need for multi-locus testing. J Mol Med (Berl) 2014: 92: 769–777.
23. Kotzot D. Complex and segmental uniparental disomy updated. J Med Genet 2008: 45: 545–556.
24. Lapunzina P, Monk D. The consequences of uniparental disomy and copy number neutral loss-of-heterozygosity during human development and cancer. Biol Cell 2011: 103: 303–317.
25. Choufani S, Shuman C, Weksberg R. Beckwith-Wiedemann syndrome. Am J Med Genet C Semin Med Genet 2010: 154C: 343–354.

RESEARCH LETTER

Circulating levels of maternal plasma cell-free miR-21 are associated with maternal body mass index and neonatal birth weight

Kiyonori Miura[1]*, Ai Higashijima[1], Yuri Hasegawa[1], Shuhei Abe[1], Shoko Miura[1], Masanori Kaneuchi[1], Koh-ichiro Yoshiura[2] and Hideaki Masuzaki[1]

[1]Department of Obstetrics and Gynecology, Nagasaki University Graduate School of Biomedical Sciences, Nagasaki, Japan
[2]Department of Human Genetics, Nagasaki University Graduate School of Biomedical Sciences, Nagasaki, Japan
*Correspondence to: Kiyonori Miura. E-mail: kiyonori@nagasaki-u.ac.jp

Funding sources: K.M., S.M., and H.M. were supported by JSPS KAKENHI (grant numbers 26462495, 24791712, and 25462563, respectively).
Conflicts of interest: None declared

Circulating cell-free microRNA (miRNA) levels in maternal plasma are involved in, or associated with, pregnancy-associated disorders, such as preeclampsia, fetal growth restriction, and preterm delivery. Therefore, they have a strong potential for use as sensitive and specific biomarkers.[1] Recently, aberrant expression of miR-21 was reported to be associated with fetal hypoxia, fetal growth restriction, and macrosomia,[2–4] suggesting that plasma miR-21 levels may be a candidate biomarker for fetal status. MiRNA-21 is expressed in maternal fetal and placenta tissues. Therefore, maternal miR-21, fetal miR-21, and placental miR-21 are circulating in maternal plasma. However, which clinical variables (maternal, fetal, or placental factors) affect the circulating levels of total miRNAs in maternal plasma remains unknown. In this study, to clarify the factors affecting the circulating levels of total miRNAs in maternal plasma, we measured plasma cell-free miR-21 levels and investigated their association with maternal body mass index (BMI) as a maternal factor, neonatal birth weight (BW) and fetal gender as a fetal factor, and placental weight (PW) as a placental factor.

All samples were obtained after receiving written informed consent, and the Institutional Review Board of Nagasaki University approved the study protocol. Women who smoked; those who had multiple gestations, placenta previa, invasive placentation, preterm labor, preeclampsia, or infection; and those with the presence of fetal anomalies or aneuploidy or fetal growth restriction were excluded. Finally, we obtained maternal blood from 52 uncomplicated pregnant women with a female singleton fetus and 30 uncomplicated pregnant women with a male singleton fetus at 37–38 weeks' gestation to exclude the possibility of preterm labor. Gestational age was assessed using ultrasonography. All of the women had nothing to eat or drink for 8 h prior to blood collection. Maternal blood samples (7 mL) were collected within 3 h of elective cesarean section. At the time of blood sampling, they had no signs of labor. Preparation and extraction of total RNA containing small RNA molecules were performed as described previously.[5–7]

All specific primers and TaqMan probe of miR-21 were purchased from TaqMan MicroRNA Assays (Applied Biosystems, Warrington, UK). Absolute qRT-PCR of miRNAs in plasma samples was performed as described previously.[5–7] For each miRNA assay, we prepared a calibration curve by tenfold serial dilution of single-stranded cDNA oligonucleotides corresponding to each miRNA sequence from 1.0×10^2 to 1.0×10^8 copies/mL. Each sample and each calibration dilution were analyzed in triplicate. Each assay could detect down to 300 RNA copies/mL [9,10].[5,6] Every batch of amplifications included three water blanks as negative controls for each of the reverse transcription and PCR steps. All of the data were collected and analyzed using the LightCycler® 480 real-time PCR system (Roche, Pleasanton, CA, USA). Pearson product–moment correlation coefficients between plasma cell-free miR-21 levels and clinical variables (BMI, BW, and PW) were analyzed with SPSS version 19 (IBM Japan, Tokyo, Japan). Significance was defined as $P < 0.05$. To eliminate spurious correlations between circulating cell-free miR-21 levels and BMI, BW, or PW, partial correction coefficient analysis was performed.

In 52 pregnant women with a female fetus, the median (minimum–maximum) cell-free miR-21 level in maternal plasma was 3.23×10^5 copies/mL (6.41×10^3–4.98×10^6 copies/mL). In 30 pregnant women with a male fetus, the median cell-free miR-21 level in maternal plasma was 1.73×10^6 copies/mL (1.14×10^5–4.75×10^6 copies/mL). There was no significant difference in plasma cell-free miR-21 levels between pregnant women bearing male and female fetuses (Mann–Whitney U-test, $P > 0.05$). In 52 pregnant women with a female fetus, the median (minimum–maximum) BMI, BW, and PW were 20.3 kg/m^2 (14.7–37.0 kg/m^2), 2849 g (2274–4040 g), and 595 g (400–870 g), respectively. No relationship was detected between BMI and PW ($r = 0.130$ and $P = 0.358$). However, significant associations

were observed between BW and PW and between BMI and BW ($r=0.731$ and $P<0.01$; $r=0.530$ and $P<0.01$, respectively). In pregnant women bearing a female fetus, plasma cell-free miR-21 levels were associated with BMI and BW but not with PW (Table 1, Figure 1a and c). In 30 pregnant women with a male fetus, the median (minimum–maximum) BMI, BW, and PW were 20.7 kg/m^2 (16.0–35.9 kg/m^2), 3075 g (2014–3616 g), and 560 g (390–900 g), respectively. No relationship was detected between BMI and PW or between BMI and BW ($r=0.351$ and $P=0.057$; $r=0.323$ and $P=0.082$, respectively). However, a significant association was observed between BW and PW ($r=0.782$ and $P<0.01$). In pregnant women bearing a male fetus, plasma cell-free miR-21 levels were associated with BMI and BW but not with PW (Table 1, Figure 1b and d).

In this study, in female and male pregnancies, we found that plasma cell-free miR-21 levels were associated with BMI and BW but not with PW. And also, circulating cell-free miR-21 levels in maternal plasma were independent of fetal gender.

Our finding of an association between plasma cell-free miR-21 levels and neonatal BW is consistent with previous data. Maccani *et al.* showed that a low expression of miR-21 in the placenta was associated with infants with growth restriction

Table 1 Summary of correlation coefficient analysis between plasma cell-free miR-21 levels and clinical variables

			Clinical variables					
			Neonatal birth weight		Maternal body mass index		Placental weight	
MiRNAs	Fetal sex	Statistical analysis	*r*-value	*P*-value	*r*-value	*P*-value	*r*-value	*P*-value
MiR-21	Female	Pearson product–moment correlation coefficient	0.616	<0.01	0.557	<0.01	0.369	<0.01
		Partial correction coefficient	0.345[a]	0.013[a]	0.300[a]	0.034[a]	−0.152[b]	0.287[b]
	Male	Pearson product–moment correlation coefficient	0.741	<0.01	0.441	0.015	0.725	<0.01
		Partial correction coefficient	0.406[c]	0.029[c]			0.347[b]	0.065[b]

[a]Placental weight and maternal body mass index were used as control variables.
[b]Neonatal birth weight was used as a control variable.
[c]Placental weight was used as a control variable.

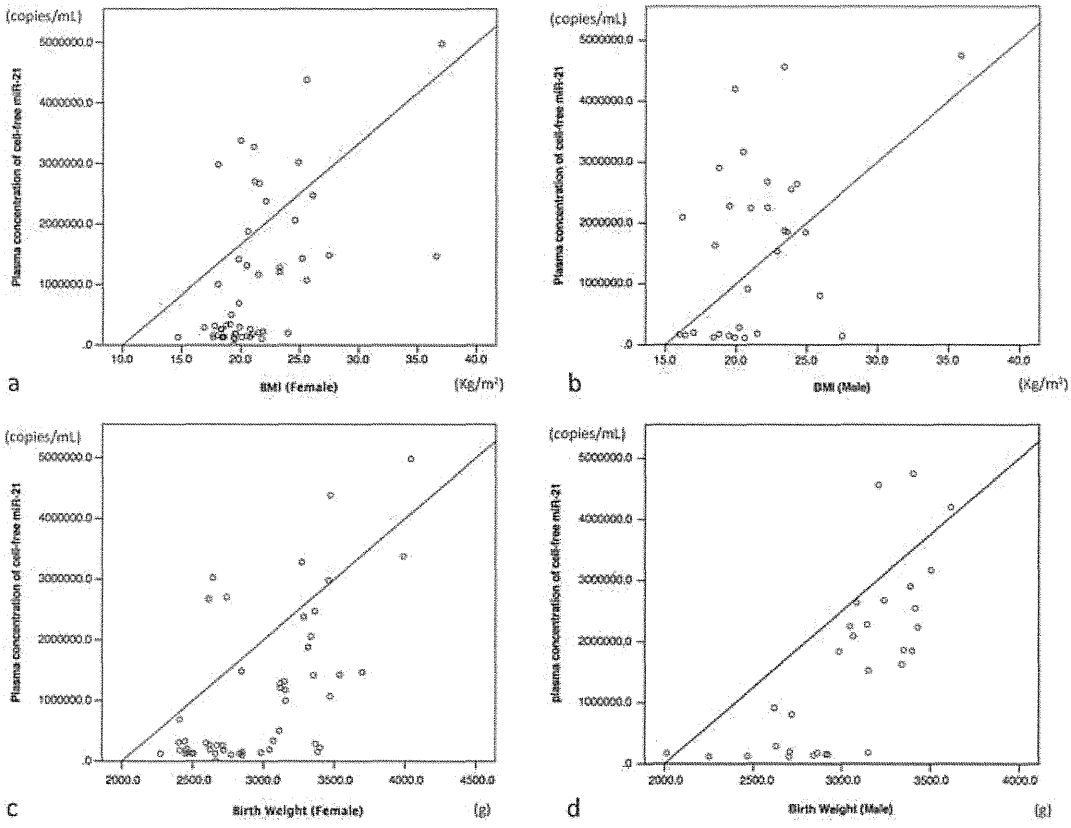

Figure 1 Graph showing relationship between plasma concentration of cell-free miR-21 and clinical variables The correlation coefficient between BMI and cell-free miR-21 levels for (a) female pregnancy is 0.300 (*P*-value: 0.034) and for (b) male pregnancy is 0.441 (*P*-value: 0.015). The correlation coefficient between birth weight and cell-free miR-21 levels for (c) female pregnancy is 0.345 (*P*-value: 0.013) and for (d) male pregnancy is 0.406 (*P*-value: 0.029)

and low BW.[3] Additionally, Jiang *et al.* reported that aberrant upregulation of miR-21 was detected in placental tissues of macrosomia.[4] Therefore, miR-21 expression levels in placental tissues appear to be associated with BW as a fetal factor. Our data and data from these previous studies[3,4] suggest that BW affects total circulating levels of cell-free miR-21 in maternal plasma.

Our finding of an association between plasma cell-free miR-21 levels and maternal BMI is consistent with previous findings of cell-free DNA in maternal plasma. Vora *et al.* showed that circulating cell-free DNA levels in maternal plasma are associated with maternal BMI, suggesting that maternal BMI affects total cell-free DNA levels in pregnant women.[8] In obese women, increased levels of total cell-free DNA may reflect increased necrosis of adipocytes and stromal vascular apoptosis.[9] Therefore, similar to the association between cell-free DNA and maternal BMI, increased plasma cell-free miRNA levels may reflect increased levels of necrosis of adipocytes and stromal vascular apoptosis. Our previous study showed that circulating levels of cell-free placenta-specific miRNAs were associated with PW but not with BMI or BW.[10] In the current study, circulating cell-free miR-21 levels, which are expressed in maternal, fetal, and placental tissues, were associated with BMI and BW but not with PW. All of the cell-free placenta-specific miRNAs in maternal plasma are of placental origin. However, the majority of total cell-free miRNAs in maternal plasma is of maternal origin, and some of them have fetal or placental origins. Therefore, BMI, as a maternal factor, affects total cell-free miR-21 levels in pregnant women.

This is the first study to investigate the association between circulating plasma cell-free miR-21 levels and clinical variables (BMI, BW, PW, and fetal gender). In female and male pregnancies, we found that increased BMI and BW were associated with higher circulating cell-free miR-21 levels in the plasma of pregnant woman, suggesting that BMI and BW affect total cell-free miR-21 levels in maternal plasma. When circulating miR-21 levels are used to estimate fetal growth, diagnose fetal hypoxia, or quantify its severity,[2] raw data of cell-free miR-21 levels in maternal plasma may need to be adjusted for maternal BMI and neonatal BW.

ACKNOWLEDGEMENTS

We would like to thank Ayako Ueyama, Shizuka Yoshii, Hiroko Sakakida, and Yasuko Noguchi for their technical assistance.

WHAT'S ALREADY KNOWN ABOUT THIS TOPIC?

- Circulating cell-free microRNA levels in maternal plasma are measurable.
- Circulating levels of some microRNAs are associated with pregnancy-associated disorders.

WHAT DOES THIS STUDY ADD?

- Cell-free miR-21 levels in maternal plasma are independent of fetal gender.
- Neonatal birth weight affects plasma cell-free miR-21 levels.
- Maternal body mass index affects plasma cell-free miR-21 levels.

REFERENCES

1. Morales-Prieto DM, Ospina-Prieto S, Chaiwangyen W, *et al.* Pregnancy-associated miRNA-clusters. J Reprod Immunol 2013;97:51–61.
2. Whitehead CL, Teh WT, Walker SP, *et al.* Circulating microRNAs in maternal blood as potential biomarkers for fetal hypoxia *in-utero*. PLoS One 2013;8:e78487.
3. Maccani MA, Padbury JF, Marsit CJ. MiR-16 and miR-21 expression in the placenta is associated with fetal growth. PLoS One 2011;6: e21210.
4. Jiang H, Wu W, Zhang M, *et al.* Aberrant upregulation of miR-21 in placental tissues of macrosomia. J Perinatol 2014;34:658–63.
5. Chim SS, Shing TK, Hung EC, *et al.* Detection and characterization of placental microRNAs in maternal plasma. Clin Chem 2008;54:482–90.
6. Miura K, Miura S, Yamasaki K, *et al.* Identification of pregnancy-associated microRNAs in maternal plasma. Clin Chem 2010;56:1767–71.
7. Higashijima A, Miura K, Mishima H, *et al.* Characterization of placenta-specific microRNAs in fetal growth restriction pregnancy. Prenat Diagn 2013;33:214–22.
8. Vora NL, Johnson KL, Basu S, *et al.* A multifactorial relationship exists between total circulating cell-free DNA levels and maternal BMI. Prenat Diagn 2012;32:912–4.
9. Haghiac M, Vora NL, Basu S, *et al.* Increased death of adipose cells, a path to release cell-free DNA into systemic circulation of obese women. Obesity (Silver Spring) 2012;20:2213–9.
10. Miura K, Morisaki S, Abe S, *et al.* Circulating levels of maternal plasma cell-free pregnancy-associated placenta-specific microRNAs are associated with placental weight. Placenta 2014;35:848–51.

5 de Perrot M, Brundler M, Totsch M, Mentha G, Morel P. Mesenteric cysts. Toward less confusion? *Dig. Surg.* 2000; **17**: 323–8.
6 Deraison C, Bonnart C, Lopez F *et al.* LEKTI fragments specifically inhibit KLK5, KLK7, and KLK14 and control desquamation through a pH-dependent interaction. *Mol. Biol. Cell* 2007; **18**: 3607–19.
7 Mihmanli I, Erdogan N, Kurugoglu S, Aksoy SH, Korman U. Radiological workup in mesenteric cysts: Insight of a case report. *Clin. Imaging* 2001; **25**: 47–9.
8 Kumar S, Agrawal N, Khanna R, Khanna AK. Giant lymphatic cyst of omentum: A case report. *Cases J.* 2009; **2**: 23.
9 Dechev IY, Zaprianov Z, Banchev AV. A rare case of epidermoid cyst of the scrotum with signs of malignization: Clinical and morphological features. *Folia Med. (Plovdiv)* 2005; **47**: 92–4.
10 Wong SW, Gardner V. Sudden death in children due to mesenteric defect and mesenteric cyst. *Am. J. Forensic Med. Pathol.* 1992; **13**: 214–16.

Neonatal case of novel *KMT2D* mutation in Kabuki syndrome with severe hypoglycemia

Yuji Gohda,[1] Shohki Oka,[1] Takamoto Matsunaga,[2] Satoshi Watanabe,[3,4] Koh-ichiro Yoshiura,[3] Tatsuro Kondoh[5] and Tadashi Matsumoto[5]

[1]*Department of Pediatrics, Sasebo Kyosai Hospital,* [2]*Obstetrics and Gynecology Matsunaga Clinic, Sasebo,* [3]*Department of Human Genetics,* [4]*Department of Pediatrics, Nagasaki University School of Medicine, Nagasaki and* [5]*Division of Developmental Disability, Misakaenosono Mutsumi Developmental, Medical, and Welfare Center, Isahaya, Japan*

Abstract A newborn Japanese girl with Kabuki syndrome had neonatal persistent hyperinsulinemic hypoglycemia, which seemed to be a rare complication of Kabuki syndrome. On sequence analysis she was found to have a novel heterozygous *KMT2D* mutation. Diazoxide therapy was effective for the hypoglycemia. Hypoglycemia should be considered when Kabuki syndrome patients have convulsion or other non-specific symptoms. Diazoxide may help to improve hypoglycemia in patients with Kabuki syndrome complicated with hyperinsulinemic hypoglycemia.

Key words diazoxide, hyperinsulinism, hypoglycemia, Kabuki syndrome, *KMT2D*.

Kabuki syndrome (KS; OMIM 147920) is a rare multiple congenital anomaly syndrome characterized by a characteristic facial anomaly, cardiac anomalies, postnatal short stature, skeletal abnormalities, and mild–moderate mental retardation. The prevalence of KS has been estimated to be 1 in 32 000 Japanese newborn infants.[1] Mutations in the *KMT2D* (*MLL2*) gene, located on chromosome 12, and the *KDM6A* (*UTX*) gene on chromosome X have been identified in KS patients.[2,3] Severe hypoglycemia is thought to be a rare complication of KS and management of this condition has not been established.[4] We describe the case of a Japanese girl with KS complicated with neonatal/persistent hyperinsulinemic hypoglycemia. Consent was obtained from the patient's parents for submission of this case report.

Case report

A female infant was born at 37 weeks gestation by spontaneous vaginal delivery to a 30-year-old G1P1 mother at a neighboring obstetrics clinic. The infant did not have asphyxia. Apgar scores at 1 and 5 min after birth were 8 and 8, respectively. The parents were not consanguineous and were healthy. Birthweight, length, and head circumference were 2544 g (–1.4 SD), 46.0 cm (–1.5 SD), and 30.5 cm (–2.0 SD), respectively. Four hours after birth, she was transferred to hospital because of tachypnea, low SpO_2 approximately 90% on room air, and severe hypoglycemia (<20 mg/dL on blood sugar test from a blood sample obtained at 2 h after birth).

Blood glucose concentration was below 1 mg/dL and vigor was decreased on admission. She was treated with 10% dextrose boluses and continuous infusion of 10% dextrose, but the hypoglycemia persisted. She then received repeated 10% dextrose boluses, i.v. injection of glucagon (0.1 mg/kg), i.v. injection of hydrocortisone (5 mg/kg), and continuous infusion of 15% dextrose. She was diagnosed with hyperinsulinemic hypoglycemia on subsequent blood examination. Laboratory data on admission were as follows: red blood cells, 5.44×10^6/μL; hemoglobin, 21.1 mg/dL; hematocrit (Hct), 72%; white blood cells, 18 940/μL (bandform neutrophil, 22%; segmented neutrophil, 40%; monocyte, 4%; lymphocyte, 34%); platelets, 111×10^3/μL; C-reactive protein, 0.01 mg/dL; IgG, 663 mg/dL; IgM, 7 mg/dL; aspartate aminotransferase, 74 U/L; alanine aminotransferase, 17 U/L; lactate dehydrogenase, 856 IU/L; blood urea nitrogen, 10.6 mg/dL; creatinine, 0.82 mg/dL; blood sugar, <1 mmol/L; insulin, 5.2 μU/mL; Na, 141.9 mEq/L; K, 4.56 mEq/L; Cl, 107.4 mEq/L; and Ca, 9.00 mg/dL. Neonatal

Correspondence: Yuji Gohda, MD, Department of Pediatrics, Sasebo Kyosai Hospital, 10-17, Shimati-cho, Sasebo 857-8575, Japan. Email: ygouda-alg@umin.ac.jp

Received 24 September 2014; revised 8 November 2014; accepted 17 November 2014.
doi: 10.1111/ped.12574

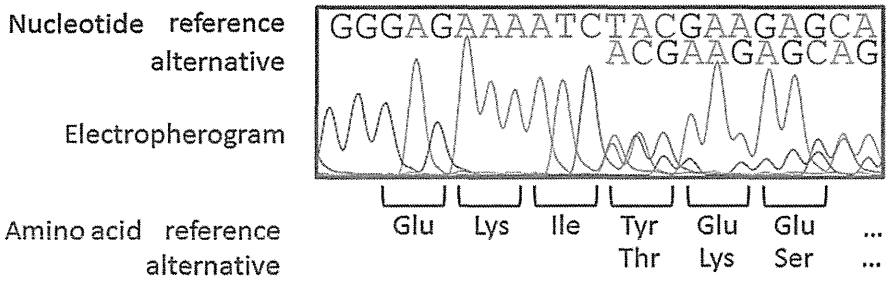

Fig. 1 Sequencing analysis of *KMT2D* in the present patient.

metabolic mass screening and tandem mass screening were within the normal range. Thyroid function was also within the normal range. The patient received partial exchange transfusion with isotonic saline twice (on days 2 and 3 of admission) because of polycythemia with Hct 80%. On day 2 of admission, insulin, total acetone, acetoacetic acid, and 3-hydroxybutyric acids were 17.8 μU/mL (normal range, 2.2–12.4 μU/mL), 17 μmol/L (normal, <131 μmol/L), 18 μmol/L (normal, <55 μmol/L), and 9 μmol/L (normal, <85 μmol/L), respectively. She also received continuous infusion of 15% dextrose and breast or formula feeding for severe hypoglycemia, but the hypoglycemia did not improve. Blood concentration of glucose was also unstable. Diazoxide treatment, 5 mg/kg/day, was started on day 29 after birth, and the dose was increased to 10 mg/kg/day on day 44 and was maintained thereafter. The severe hypoglycemia gradually improved. Laboratory data on day 44 were as follows: blood sugar, 2.3 mmol/l; insulin, 2.6 μU/mL; total acetone, 62 μmol/L; acetoacetic acid, 18 μmol/L; 3-hydroxybutyric acid, 44 μmol/L; and free fatty acid, 0.24 mEq/L (normal, 0.10–0.81 mEq/L).

The patient had dysmorphic characteristics including prominent forehead, asymmetric facial appearance, long palpebral fissures, eversion of lower eyelids, broad arched sparse eyebrows, broad depressed nasal tip, large prominent ears, and a fingertip pad on all fingers. She also had a septal atrial defect of 7.5 mm × 11.5 mm in area, bilateral breast development, recurrent otitis media, and bilateral hearing loss. She was diagnosed with KS from these clinical features. Weight, height, and head circumference at 18 months old were 8.2 kg (−1.5 SD), 76.5 cm (−0.75 SD), and 43.3 cm (−2.2 SD), respectively. Developmental quotient on Enjoji scale in total, motor, society and speech areas at 18 months old was 46, 58, 47, and 33, respectively.

Next generation sequencer screening

Genomic DNA was isolated from lymphocytes. DNA extraction was performed using QIAamp® DNA Mini Kit (Qiagen, Düsseldorf, Germany) according to the manufacturer's protocol.

Ion Proton sequencer and AmpliSeq Custom Panel (LifeTechnologies, Carlsbad, CA, USA) were used to search for mutations in *KMT2D* and *KDM6A*, which cause KS. A sequence library was prepared using Ion AmpliSeq Library kit 2.0 (LifeTechnologies) according to the manufacturer's protocol. Ion One Touch 2 (LifeTechnologies) was used to perform multiplex emulsion polymerase chain reaction, and sequence data were obtained using the IonProton sequencer. Next, sequence data were processed with Torrent Suite (LifeTechnologies), and mutations were called by Variant Caller according to the manufacturer's protocol. Single-nucleotide variants and insertions/deletions were annotated with ANNOVAR (http://www.openbioinformatics.org/annovar/). The mutation was confirmed on direct sequencing using capillary sequencer Genetic Analyzer 3130*xl* (Applied Biosystems, Foster City, CA, USA).

Mutation in KMT2D

A deletion mutation, c.16327delT, pY5443fs, was identified in exon 51 of *KMT2D* in this patient and was validated on direct sequencing (Fig. 1). This mutation generates a frameshift and was classified as the truncation type. Because the mutation found in KS is often classified as the truncation type, we thought that this base change was responsible for causing the disease. This is a novel mutation.

Discussion

Kabuki syndrome is diagnosed clinically on the combination of five main criteria: (i) postnatal growth retardation; (ii) developmental/mental disability; (iii) typical facial features; (iv) skeletal anomalies; and (v) fingertip pads.[1,4,5] The present patient had the typical facial features, fingertip pads, and developmental delay, although growth retardation and skeletal findings were not clear.

Hypoglycemia is not a major complication of KS, although it has been noted in some reports.[4,6] Neonatal hypoglycemia is divided into the transient and persistent types, and the former is considered non-hereditary.[7] Hyperinsulinemic hypoglycemia, caused by dysfunction of the ATP-dependent potassium channel due to a mutation in *ABCC8* or *KCNJ11*, is the most common type of persistent hypoglycemia. If adequate treatment is not carried out, the patient will have serious neurologic sequelae such as convulsions, developmental delay, and/or cerebral palsy. Diazoxide therapy is the first choice of treatment for hyperinsulinemic hypoglycemia and tends to maintain an adequate blood sugar level, especially in patients with the persistent type of hypoglycemia.

The rate of neonatal hypoglycemia among KS patients is 21/313 (6.7%).[4] Among these KS patients, four had had persistent hypoglycemia and only one was suspected of having hyperinsulinism.[4] Three different KS patients with hyperinsulinemic hypoglycemia were treated with diazoxide (Table 1): two patients aged 9 months and 3 years old in the reports had continued diazoxide therapy, and the remaining one patient was able

Table 1 Persistent hypoglycemia in patients with Kabuki syndrome

Characteristics	Patient[ref no.]					Present patient
	1[8]	2[8]	3[8]	4[8]	5[5]	
Age of onset	Day 1	Day 1	Day 1	Day 1	NM	Day 1
Symptoms	Seizure	Jitteriness	Poor feeding	Poor feeding	NM	Vigor defect
Blood sugar (mmol/L)	2.4	2.5	2.3	2.9	NM	<1.0
Insulin (mU/L)	22	3.9	42.3	<2	NM	17.8
Cause of hypoglycemia	Hyperinsulinism	Hyperinsulinism	Not known	GH deficiency	Hyperinsulinism	Hyperinsulinism
Treatment	Diazoxide+ Chlorothiazide	Diazoxide+ Chlorothiazide	Feeding regimen	GH	Diazoxide	Diazoxide
KMT2D mutation	Negative, c.12964C>T	c.6971dupC, c.10101G>T	c.5845C>T	c.2992C>G	c.9931C>T	c.16327delT

GH, growth hormone; NM, not mentioned.

to stop this therapy at 5 years old.[5,8] The present patient started diazoxide therapy on day 29 after birth and has continued to take this drug at the time of writing. In each case, hypoglycemia was not seen after diazoxide therapy was started; thus, diazoxide therapy would be effective in KS patients, although the prognosis of KS patients with severe hypoglycemia is not known.

On gene analysis of the aforementioned three KS patients, two patients had *KMT2D* mutations (c.6971dupC [p.D2325X], heterozygote, and c.9931C>T [p.L3367X)]; Table 1). The third patient did not have a mutation in *KMT2D*.[5,8] The present KS patient had a novel heterozygous *KMT2D* mutation of c.16327delT (p.Y5443fs). *KMT2D* encodes a large protein containing the SET domain. KMT2D is a transcriptional activator that induces the transcription of target genes by covalent histone modification and that appears to be involved in the regulation of adhesion-related cytoskeletal events, which might affect cell growth and survival.[9] It is unknown, however, whether the function of KMT2D is related to pancreatic insulin secretion or not. Furthermore, the correlation between genotype and hypoglycemia is not clear because these three KS patients had different kinds of mutations across *KMT2D*. Among 20 KS patients with a *KDM6A* mutation, hypoglycemia was observed in six patients and hyperinsulinism in one patient.[3] *KDM6A* mutation may also cause hyperinsulinemic hypoglycemia as well as other KS manifestations of developmental/mental delay, characteristic facies, dermatographic features and so on, because KMT2D associates with KDM6A and they are important for the stringent regulation of transcription during cellular differentiation.[10]

Conclusion

We have reported a female KS patient with typical dysmorphic features and developmental delay and a novel *KMT2D* mutation. She was complicated with severe hypoglycemia with hyperinsulinism that may be an important complication of KS. Hypoglycemia should be considered when KS patients have convulsion or other non-specific symptoms, such as jitteriness or feeding difficulty. Hyperinsulinism may be an important cause of hypoglycemia. Diazoxide could help to improve hypoglycemia in patients with KS complicated with hypoglycemia.

Acknowledgment

The authors state that they have no conflicts of interest.

References

1 Niikawa N, Kuroki Y, Kajii T *et al.* Kabuki make-up (Niikawa-Kuroki) syndrome: A study of 62 patients. *Am. J. Med. Genet.* 1988; **31**: 565–89.
2 Ng SB, Bigham AW, Buckingham KJ *et al.* Exome sequencing identifies MLL2 mutations as a cause of Kabuki syndrome. *Nat. Genet.* 2010; **42**: 790–93.
3 Banka S, Lederer D, Benoit V *et al.* Novel *KDM6A* (UTX) mutations and a clinical and molecular review of the X-linked Kabuki syndrome (KS2). *Clin. Genet.* 2014. doi:10.1111/cge.12363. [Epub ahead of print].
4 Genevieve D, Amiel J, Viot G *et al.* Atypical findings in Kabuki syndrome: Report of 8 patients in a series of 20 and review of the literature. *Am. J. Med. Genet.* 2004; **129A**: 64–8.
5 Zarate YA, Zhan H, Jones JR. Infrequent manifestations of Kabuki syndrome in a patient with novel MLL2 mutation. *Mol. Syndromol.* 2012; **3**: 180–84.
6 Ewart-Toland A, Enns GM, Cox VA, Mohan GC, Rosenthal P. Severe congenital anomalies requiring transplantation in children with Kabuki syndrome. *Am. J. Med. Genet.* 1998; **80**: 362–7.
7 Fournet JC, Junien C. Genetics of congenital hyperinsulinism. *Endocr. Pathol.* 2004; **15**: 233–40.
8 Subbarayan A, Hussain K. Hypoglycemia in Kabuki syndrome. *Am. J. Med. Genet. A* 2014; **164A**: 467–71.
9 Issaeva I, Zonis Y, Rozovskaia T *et al.* Knockdown of ALR (MLL2) reveals ALR target genes and leads to alterations in cell adhesion and growth. *Mol. Cell. Biol.* 2007; **27**: 1889–903.
10 Agger K, Cloos PA, Christensen J *et al.* UTX and JMJD3 are histone H3K27 demethylases involved in HOX gene regulation and development. *Nature* 2007; **449**: 731–4.

Clinical Immunology 160 (2015) 255–260

Contents lists available at ScienceDirect

Clinical Immunology

journal homepage: www.elsevier.com/locate/yclim

Brief Communication

Novel compound heterozygous *DNA ligase IV* mutations in an adolescent with a slowly-progressing radiosensitive-severe combined immunodeficiency

Shinobu Tamura [a,1], Kohei Higuchi [b], Masaharu Tamaki [a], Chizuko Inoue [c], Ryoko Awazawa [d], Noriko Mitsuki [e], Yuka Nakazawa [f,g,h], Hiroyuki Mishima [i], Kenzo Takahashi [d], Osamu Kondo [b], Kohsuke Imai [e], Tomohiro Morio [e], Osamu Ohara [j], Tomoo Ogi [f,g,h], Fukumi Furukawa [k], Masami Inoue [b], Koh-ichiro Yoshiura [i], Nobuo Kanazawa [k,*,1]

[a] *Department of Hematology and Oncology, Kinan Hospital, Wakayama, Japan*
[b] *Department of Hematology and Oncology, Osaka Medical Center and Research Institute for Maternal and Child Health, Osaka, Japan*
[c] *Sarashi Clinic, Wakayama, Japan*
[d] *Department of Dermatology, University of the Ryukyus, Okinawa, Japan*
[e] *Department of Pediatrics, Tokyo Medical and Dental University, Tokyo, Japan*
[f] *Nagasaki University Research Centre for Genomic Instability and Carcinogenesis, Nagasaki University, Nagasaki, Japan*
[g] *Department of Genome Repair, Nagasaki University Graduate School of Biomedical Sciences, Nagasaki, Japan*
[h] *Department of Genetics, Research Institute of Environmental Medicine, Nagoya University, Nagoya, Japan*
[i] *Department of Human Genetics, Atomic Bomb Disease Institute, Nagasaki University, Nagasaki, Japan*
[j] *Department of Technology Development, Kazusa DNA Research Institute, Kisarazu, Japan*
[k] *Department of Dermatology, Wakayama Medical University, Wakayama, Japan*

ARTICLE INFO

Article history:
Received 8 April 2015
Received in revised form 5 July 2015
Accepted with revision 6 July 2015
Available online 11 July 2015

Keywords:
DNA ligase IV
Hematopoietic stem cell transplantation
LIG4 syndrome
Severe combined immunodeficiency
TREC/KREC
Whole exome sequencing

ABSTRACT

We herein describe a case of a 17-year-old boy with intractable common warts, short stature, microcephaly and slowly-progressing pancytopenia. Simultaneous quantification of T-cell receptor recombination excision circles (TREC) and immunoglobulin κ-deleting recombination excision circles (KREC) suggested very poor generation of both T-cells and B-cells. By whole exome sequencing, novel compound heterozygous mutations were identified in the patient's *DNA ligase IV* (*LIG4*) gene. The diagnosis of LIG4 syndrome was confirmed by delayed DNA double-strand break repair kinetics in γ-irradiated fibroblasts from the patient and their restoration by an introduction of wild-type *LIG4*. Although the patient received allogeneic hematopoietic stem cell transplantation from his haploidentical mother, he unfortunately expired due to an insufficiently reconstructed immune system. An earlier definitive diagnosis using TREC/KREC quantification and whole exome sequencing would thereby allow earlier intervention, which would be essential for improving long-term survival in similar cases with slowly-progressing LIG4 syndrome masked in adolescents.

1. Introduction

Non-homologous DNA end joining (NHEJ) is a pathway that repairs double-strand DNA breaks (DSB) and consists of 6 components; Ku70, Ku80, DNA-PK, Artemis, XRCC4 and DNA ligase IV (LIG4) [1]. This pathway is essential for human V(D)J recombination and is involved in the development of lymphocytes [1–4]. Therefore, patients with mutations in NHEJ genes are unable to produce functional T-cells and B-cells, and suffer from primary immunodeficiency disease (PID), especially severe combined immunodeficiency disease (SCID). In addition, NHEJ genetic mutations lead to oncogenic transformation such as the development of leukemias and lymphomas [5,6].

Among the NHEJ genes, LIG4 plays pivotal roles in lymphocyte development, maintenance of hematopoietic stem cells and neurogenesis [7–9]. Loss-of-function mutations in the *LIG4* gene cause a rare SCID called LIG4 syndrome (Online Mendelian Inheritance in Man #606593), which is typically accompanied by developmental delays, pancytopenia, and radiosensitivity [10,11]. Twenty-seven cases

Abbreviations: DSB, double-strand DNA breaks; G-CSF, granulocyte-colony-stimulating factor; GvHD, graft-versus host disease; HSCT, hematopoietic stem cell transplantation; Ig, immunoglobulin; KREC, immunoglobulin κ-deleting recombination excision circles; LIG4, DNA ligase IV; NHEJ, non-homologous DNA end joining; PCR, polymerase reaction chain; PID, primary immunodeficiency disease; SCID, severe combined immunodeficiency disease; SNV, single nucleotide variation; TAC, tacrolimus; TCR, T-cell receptor; TREC, T-cell receptor recombination excision circles; WHIM, warts, hypogammaglobulinemia, infections and myelokathexis.

* Corresponding author at: Department of Dermatology, Wakayama Medical University, 811-1 Kimiidera, Wakayama, Japan.
E-mail address: nkanazaw@wakayama-med.ac.jp (N. Kanazawa).

[1] These authors contributed equally to this work.

http://dx.doi.org/10.1016/j.clim.2015.07.004
1521-6616/

with LIG4 syndrome have been reported so far in the literature [10–14]. The first identified case developed leukemia with radiosensitivity at age 14 without other clinical abnormalities [12]. However, subsequently reported cases have shown growth/developmental delays with microcephaly and unusual facial characteristics, and pancytopenia with mild immunodeficiency [10]. One of them showed extensive plantar warts. Recently reported cases have shown extensive growth failure and pancytopenia with previously unrecognized immunodeficiency later in childhood [11]. In contrast, some cases with early-onset SCID were also reported without overt developmental delays [13,14]. Thus, the clinical features of LIG4 syndrome are highly variable. In cases with progressive cytopenia and immune dysfunction, the application of allogeneic hematopoietic stem cell transplantation (HSCT) should be considered [11].

In this report, we describe an adolescent with LIG4 syndrome diagnosed using quantification of T-cell receptor recombination excision circles (TREC) and immunoglobulin (Ig) κ-deleting recombination excision circles (KREC) and whole exome sequencing. Moreover, his clinical course including a T cell receptor (TCR) $\alpha\beta^+$ T-cell and $CD19^+$ B-cell depleted haploidentical HSCT from his maternal donor is also presented herein.

2. Material and methods

2.1. Clinical and laboratory findings of the patient

A 17-year-old male Japanese adolescent consulted a hematologist because of pancytopenia (Table 1). His physical characteristics included short stature (−2 SD) and mild microcephaly, without apparent mental retardation. He had been diagnosed with an IgA deficiency at 2 years of age, but had not received treatment or medical follow-up for his condition. He was vaccinated only with Bacille–Calmette–Guerin and had a history of severe herpes infections and serous otitis media. Since 8 years of age, warts had expanded on his hands and feet in spite of various treatments given at a dermatology clinic (Fig. 1, A). Polymerase chain reaction (PCR)-based genotyping of human papilloma virus revealed the presence of the common 57c variant. He additionally showed skin-colored slightly elevated annular nodules on his trunk, which histologically consisted of epithelioid cell granuloma without evidence of infection (Fig. 1, B). A blood test at the initial visit showed low counts of white blood cells, neutrophils, lymphocytes, and platelets (Table 1). In addition, hypogammaglobulinemia, low counts of T-cells and B-cells in his blood, and a significantly low level of phytohaemagglutinin-stimulated lymphocyte blastoid transformation were also observed. Initially, warts, hypogammaglobulinemia, infections and myelokathexis (WHIM) syndrome was suspected by his clinical characteristics and also according to the algorithm for the diagnosis of PID with warts [15,16]. However, T1-weighted magnetic resonance imaging demonstrated a heterogeneous, mottled appearance of vertebral bodies and a bone marrow biopsy showed hypocellular and fatty changes without chromosomal abnormalities (Fig. 1, C).

2.2. DNA isolation and Sanger sequencing

Our patient and his mother were enrolled in this study. All experiments were performed after obtaining written informed consent from both subjects, and were approved by the Institutional Review Board of Wakayama Medical University, Tokyo Medical and Dental University and Nagasaki University in accordance with the Declaration of Helsinki. Genomic DNA was isolated using Wizard Genomic DNA Purification Kits (Promega Corporation, Fitchburg, WI). Protein-coding exons including exon-intron junctions for *CXCR4*, *RAG1*, *RAG2*, *STAT1*, *GATA2* and *LIG4* genes were amplified by PCR from genomic DNA and subjected to capillary DNA sequencing on ABI 310, 3130 or 3730 genetic analyzer (Thermo Fisher Scientific Inc., Waltham, MA) with the BigDye Terminator v3.1 Cycle Sequencing Kits (Thermo Fisher Scientific Inc.).

2.3. Quantification of TREC and KREC

TREC and KREC levels in peripheral blood were measured by real-time PCR as previously described [17,18]. The following primer pairs and probes were used: TREC forward primer (5′-CAC ATC CCT TTC AAC CAT GCT-3′) and reverse primer (5′-TGC AGG TGC CTA TGC ATC A-3′) with the probe (5′-FAM-ACA CCT CTG GTT TTT GTA AAG GTG CCC ACT TAMRA-3′) and KREC forward primer (5′-TCC CTT AGT GGC ATT ATT TGT ATC ACT-3′) and reverse primer (5′-AGG AGC CAG CTC TTA CCC TAG AGT-3′) with the probe (5′-HEX-TCT GCA CGG GCA GCA GGT TGG-TAMRA-3′). A range of more or less than 100 copies/μg DNA is defined as positive or undetectable, respectively.

2.4. Whole exome sequencing and data analysis

Exon fragments were enriched from genomic DNA samples from a patient and his mother using the SureSelect Human All Exon V4 + UTRs kits (Agilent Technologies, Santa Clara, CA), according to the manufacturer's instructions. Libraries were sequenced by a 5500 SOLiD sequencer (Thermo Fisher Scientific Inc.), to obtain 50 bp and 25 bp paired-end reads. The reads were mapped by NovoalignCSMPI version 1.02.02 (Novocraft Technologies Sdn Bhd, Selangor, Malaysia) on the hg19 human reference genome. Base quality scores of the reads were recalibrated using dbSNP135 single nucleotide variation (SNV) information during mapping. Mapped reads were subjected to marking of PCR duplication by the MarkDuplicates tools of the Picard tools package on http://broadinstitute.github.io/picard/. The Genome Analysis Toolkit

Table 1
Laboratory characteristics of the patient during follow-up.

Laboratory characteristics (normal range)	3 years before first visit (14 years old)	3 months before first visit	First visit (17 years old)	Just before HSCT (18 years old)	3 months after HSCT	1 month before his expiration (19 years old)
WBC (3.9–9.8 × 10^9/L)	2.6	1.2	0.9	2.0[a]	3.6	1.3
Hb (13.5–17.6 g/dL)	12.2	13.5	12.9	8.5[b]	11.1	10.3[b]
Platelets (15–40 × 10^9/L)	8.9	7.5	5.3	1.9[b]	18.2	4.8
ALC (1.5–4.0 × 10^9/L)	0.36	0.38	0.28	0.12	0.43	0.15
ANC (2.0–7.5 × 10^9/L)	1.98	0.76	0.26	1.52	2.26	1.14
$CD3^+$ (547–2155/μL)	NA	NA	68	74	NA	2
$CD4^+$ (344–1289/μL)	NA	NA	33	30	NA	1
$CD8^+$ (110–1066/μL)	NA	NA	80	50	NA	45
$CD19^+$ (77–470/μL)	NA	NA	1	NA	NA	2
IgG (8.48–18.18 g/L)	9.43	NA	6.71	9.87[c]	9.06[c]	5.21[c]
IgA (1.05–3.92 g/L)	<0.15	NA	<0.15	<0.15[c]	<0.15[c]	0.48[c]
IgM (0.37–1.97 g/L)	0.77	NA	0.30	0.20[c]	<0.05[c]	0.21[c]

ALC, absolute lymphocyte count; ANC, absolute neutrophil count; NA, not available; Hb, hemoglobin; HSCT, hematopoietic stem cell transplantation; WBC, white blood cells.
[a] He was supported by G-CSF subcutaneously.
[b] He received regular red blood cell and platelet transfusions.
[c] He received regular intravenous immunoglobulin therapy.

was used for the following local realignment to obtain SNV and small insertion/deletion calls combined with an in-house workflow management tool [19,20]. Called variants were sorted by comparison of data from the patient and his mother using an in-house tool and annotated with ANNOVAR software [21]. Finally, variants meeting the following criteria were selected as deleterious mutations: 1) causing stop gain, stop loss, non-synonymous mutation, or splice site mutation; 2) alternative allele frequencies in databases (Complete Genomics' whole genome data of 69 individuals, the 1000 genomes project, and an in-house database) are all equal to or less than 0.5%; and 3) not included in Segmental duplication region defined in the UCSC genome browser [22,23].

2.5. Gamma-H2AX assay

Primary skin fibroblasts were X-ray irradiated at a dose of 3 Gy and γ-H2AX foci were visualized by staining with monoclonal anti-γ-H2AX (Merk Millipore, Billerica, MA) and subsequent secondary antibodies (Thermo Fisher Scientific Inc.). Cell nuclei were counterstained with 4,6-diamidino-2-phenylindole and foci were quantified using a high content cell imaging system at the indicated time points. For complementation assays, patient-derived fibroblasts were infected with lentivirus expressing the wild-type *LIG4* cDNA or mock-treated and provided for irradiation as described elsewhere [24].

3. Results

3.1. Demonstration of a phenotype of T^-B^- SCID by TREC/KREC quantification

Simultaneous measurement of TREC and KREC copy numbers in peripheral blood can readily identify patients with SCID and other PIDs [17,18]. In our patient, an absence of mutations in the responsible *CXCR4* gene finally excluded a diagnosis of WHIM syndrome and quantification of TREC and KREC in his peripheral blood was conducted six months after the initial visit [15]. The results revealed the titer of TREC in the lower limit of normal (298 versus $8.2 \pm 6.3 \times 10^2$ copies/μg DNA in 13 to 18-year-old control children) and an undetectable titer of KREC (58 versus $3.6 \pm 3.8 \times 10^3$ copies/μg DNA in 7 to 18-year-old control children), suggesting the presence of SCID with defective T-cell and B-cell development (Fig. 1, D) [17,18].

3.2. Identification of novel compound heterozygous mutations of the LIG4 gene by whole exome sequencing

The absence of mutations in *RAG1*, *RAG2*, *STAT1*, and *GATA2*, which are known as causative genes associated with SCID, in the patient's genomic DNA led us to perform whole exome sequencing of the patient's and his mother's genomic DNA. More than 200 novel mutations were picked up as candidates in both recessive and dominant inheritance models (Supplementary Table 1). Among them, compound heterozygous mutations in the *LIG4* gene, c.1237G>T causing the truncation p.E413* and c.1341G>T causing the substitution p.W447C were identified in the patient (Fig. 1, E). Only the former truncating mutation was detected in his mother. Furthermore, only one mutation was detected in each clone of the PCR-amplified and subcloned patient's DNA fragments containing both nucleotides at 1237 and at 1341 of *LIG4*, which confirmed the compound heterozygosity of the two mutations (data not shown). Indeed, no report has described these two mutations in the *LIG4* gene [11]. However, they arise within the enzymatic domain and a tryptophan residue at position 447, which is highly conserved among species, comprises the active site of the adenylation domain of LIG4 (cd07903 in NCBI's conserved domain database), predicting their functional significance (Fig. 1, F). Examination of their ligase activities, which can directly show their functional abnormalities, has not been performed.

3.3. Delayed DSB repair kinetics in fibroblasts from the patient and their restoration by an introduction of wild-type LIG4

To reveal the functional significance of these novel mutations, DSB repair kinetics in primary fibroblasts were analyzed after ionizing irradiation. With this objective, nuclear foci of phosphorylated histone H2AX called γ-H2AX, were visualized and quantified, as H2AX is phosphorylated in rapid response to irradiation-induced DSB and recruits DNA repair proteins to form the γ-H2AX foci [25]. As shown in Fig. 1, G, delayed DSB repair kinetics were observed in fibroblasts from the patient, compared with his mother's and wild-type fibroblasts. Furthermore, ectopic expression of wild-type *LIG4* cDNA in the patient cells restored normal DSB repair kinetics (Fig. 1, H). These results confirmed the pathogenicity of the newly identified *LIG4* mutations and the diagnosis of LIG4 syndrome in the patient.

3.4. Unsuccessful HSCT to the patient

The patient's pancytopenia and hypogammaglobulinemia had steadily progressed, and he required regular blood cell and platelet transfusions 8 months after the first visit (Table 1). Despite regular administration of granulocyte-colony-stimulating factor (G-CSF), high-dose intravenous Ig and other prophylactic medications, he repeatedly suffered from either serous otitis media or necrotizing ulcerative gingivitis. Owing to such progressive bone marrow failure and immunodeficiency, a HSCT was planned as curative. As neither an HLA-matched donor nor suitable cord blood were available, $TCR\alpha\beta^+$ T cell- and $CD19^+$ B cell-depleted peripheral blood HSCT from his haploidentical mother (4.65×10^6 $CD34^+$ cells/kg, 5.78×10^5 $TCR\alpha\beta^+$ cells/kg) was applied to him when he was 18 years of age. The conditioning regimen excluded total body irradiation, while including fludarabine, cyclophosphamide and anti-thymocyte globulin [26,27]. For prevention of graft-versus host disease (GvHD), tacrolimus (TAC) was given from day −1 until day 60 [28]. He showed rapid engraftment without any toxicity or GvHD and 100% blood chimerism was observed on day 60. He was discharged safely about 3 months after the HSCT. However, one month after the termination of TAC, watery diarrhea and hematochezia appeared and a colonoscopy on day 120 showed localized ulceration and hemorrhage in the terminal ileum, which were histologically compatible with GvHD. In spite of the administration of TAC and low-dose prednisolone, pancytopenia gradually developed and regular transfusions, administration of G-CSF, and intravenous Ig were required around day 180. Ten months after the transplantation, the warts on his hands and feet gradually worsened. Although his peripheral blood chimerism was 100% donor-type, the reconstitution of both T-cells and B-cells was not observed at the same time. At an age of 19 years, about 12 months posttransplantation, the patient finally died because of an insufficiently reconstituted immune system followed by a BK viral infection and subsequent acute kidney injury. The temporal change of the patient's laboratory data is summarized in Table 1.

4. Discussion

To date, only 27 cases of LIG4 syndrome have been reported, of which only four cases described adolescents [11,12,29]. Two adolescent cases had early-truncating mutations, which occurred in the enzymatic domain of both alleles. In both cases, hematological malignancies developed with poor prognoses [12,29]. The other two adolescent cases were females who survived [11]. Although both cases demonstrated growth failure and pancytopenia, which are features of LIG4 syndrome, peripheral T-cell counts were approximately 600/μL. Therefore, their infections were mild and these cases were categorized as leaky SCID [11]. In these cases, only a mutation in one allele was within the enzymatic domain and the other was a late-truncating mutation in the XRCC4-binding domain. Thus, the degree of LIG4 protein truncation is assumed to be related to the severity of growth failure and immunodeficiency, and is also

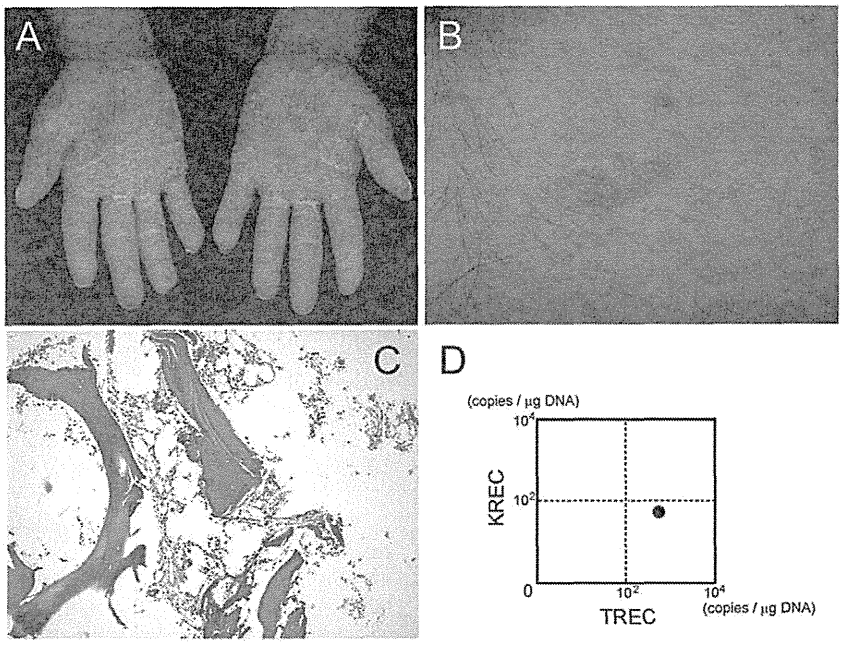
A
B
C
D
(copies / μg DNA)
KREC
TREC
(copies / μg DNA)

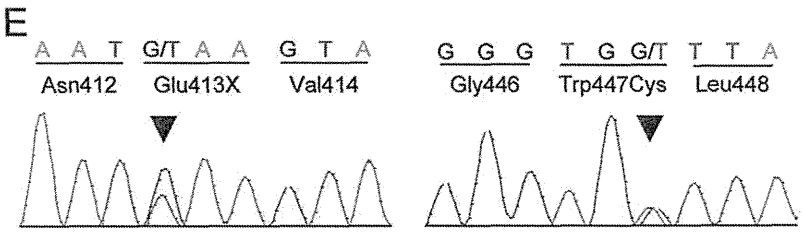
E
A A T G/T A A G T A
Asn412 Glu413X Val414
G G G T G G/T T T A
Gly446 Trp447Cys Leu448


F
Human
Mouse
Fish
Fly
Plant
Yeast
Nematode

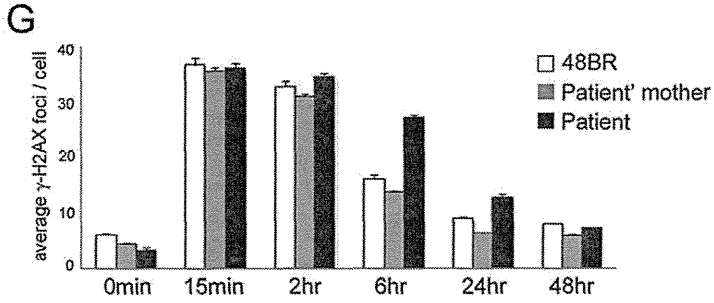
G
average γ-H2AX foci / cell
48BR
Patient' mother
Patient
0min
15min
2hr
6hr
24hr
48hr

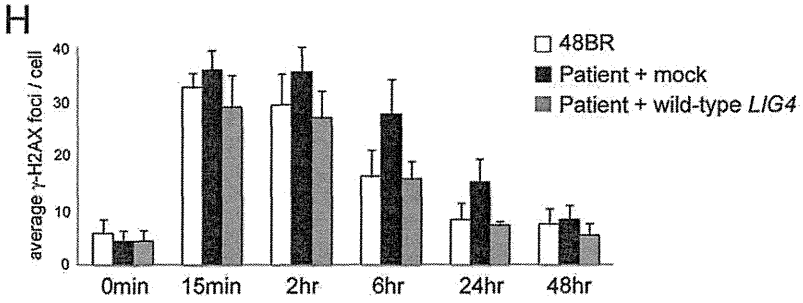
H
average γ-H2AX foci / cell
48BR
Patient + mock
Patient + wild-type LIG4
0min
15min
2hr
6hr
24hr
48hr